

Assessing the performance of open-source, semi-automated pattern recognition software for harbour seal (*P. v. vitulina*) photo ID

Izzy Langley^{1*}, Emily Hague^{1,2} and Mònica Arso Civil¹

¹Sea Mammal Research Unit, Scottish Oceans Institute, University of St Andrews, St Andrews, Scotland, UK.

²Institute of Life and Earth Sciences, Heriot-Watt University, Edinburgh, Scotland, UK.

*il32@st-andrews.ac.uk (ORCID ID: 0000-0002-8957-1373)

Acknowledgements

Data collection was funded by the Scottish Government (grant number MMSS/002/15). The authors would like to thank the expert knowledge and assistance of collaborators at each of the study sites around Scotland, without whom data collection would not have been possible.

The authors would also like to thank the publishers of all three pattern recognition software programmes for making them freely available; particularly Lex Hiby from Conservation Research Ltd. who has provided training and advice over the years. We would also like to thank the two anonymous reviewers whose comments helped to improve this manuscript.

This work is dedicated to Andy Law – a brilliant naturalist, photographer, colleague, and friend.

36 **Abstract**

37 Photographic identification (photo ID) is a well-established, non-invasive, and relatively cost-
38 effective technique to collect longitudinal data from species that can be individually
39 recognised based on natural markings. This method has been improved by computer-
40 assisted pattern recognition software which speed up the processing of large numbers of
41 images. Freely available algorithms exist for a wide range of species, but the choice of
42 software can have significant effects on the accuracy of individual capture histories and
43 derived demographic parameter estimates. We tested the performance of three open
44 source, semi-automated pattern recognition software algorithms for harbour seal (*Phoca*
45 *vitulina vitulina*) photo ID: ExtractCompare, I³S Pattern and Wild-ID. Performance was
46 measured as the ability of the software to successfully score matching images higher than
47 non-matching images using the cumulative density function (CDF). The CDF for the top
48 ranked potential match was highest for Wild-ID (CDF₁ = 0.34-0.58), followed by
49 ExtractCompare (CDF₁ = 0.24-0.36) and I³S Pattern (CDF₁ = 0.02-0.3). This trend emerged
50 regardless of how many potential matches were inspected. The highest performing aspects
51 in ExtractCompare were left heads, whereas in I³S Pattern and Wild-ID these were front
52 heads. Within each aspect, images collected using a camera and lens performed higher than
53 images taken by a camera and scope. Data processing within ExtractCompare took >4x
54 longer than Wild-ID, and >3x longer than I³S Pattern. We found that overall, Wild-ID
55 outperformed both ExtractCompare and I³S Pattern under tested scenarios, and we
56 therefore recommend its assistance in harbour seal photo ID.

57

58 **Keywords**

59 Pattern recognition; photo ID; software comparison; harbour seal; *Phoca vitulina vitulina*;
60 Wild-ID

61

62

63

64

65

66

67

68

69

70

71

72

73

74

75

76 Introduction

77 Recognising individual animals is an important tool in the monitoring of wild populations (e.g.
78 Wells and Scott 1990; Rotella et al. 2012; Letcher et al. 2015). For many species, individuals
79 are artificially marked using a wide range of techniques, including bird ringing (e.g. spotted
80 owl *Strix occidentalis*; Zimmerman et al. 2007), freeze-branding (e.g. *Chiroptera* spp;
81 Sherwin et al. 2002), colour-marking (e.g. *Satyrinae* spp; Morton 1982) and tagging (e.g.
82 pink abalone *Haliotis corrugate*; Button and Rogers-Bennet 2011). However, for some
83 species individuals can be distinguished from one another from natural markings such as
84 patterning and/or scarring (e.g. Asian elephant *Elephas maximus*; Goswami et al. 2007;
85 whale shark *Rhincodon typus*; Bradshaw et al. 2007; wild horse *Equus ferus*; Vernes et al.
86 2009). These species can be photographed and, if the image is of sufficient quality,
87 individuals can be identified. Photographic identification (photo ID) is a widely used, non-
88 invasive and relatively cost-effective method to study the distribution and life-history
89 parameters of wild populations (e.g. Thompson et al. 2008; Mackey et al. 2008; Gore et al.
90 2016; Langley et al. 2020).

91 A number of phocid seal species have individually unique pelage patterns which remain
92 stable through adulthood, enabling populations to be monitored long-term through photo ID
93 (e.g. grey seal *Halichoerus grypus*; Hiby et al. 2007; Saimaa ringed seal *Pusa hispida*
94 *saimensis*; Koivuniemi et al. 2016; harbour seal *Phoca vitulina*; Yochem et al. 1990). While
95 there is slight variation in the pelage colour and spot density among harbour seal sub-
96 species, it is not consistent enough to confidently identify to sub-species level (Kelly 1981;
97 Cunningham 2009; McCormack 2015). The repeated identification of individuals within
98 species has been successful for three of these harbour seal sub-species: *P. v. richardii* in
99 the northeast Pacific (Yochem et al. 1990), *P. v. concolor* in the northwest Atlantic
100 (McCormack 2015), and *P. v. vitulina* in the northeast Atlantic (Cunningham 2009).

101 The matching efficiency and error rates of photo ID studies have been improved by the
102 introduction of computer-assisted pattern recognition software (Arzoumanian et al. 2005;
103 Caiafa et al. 2005; Morrison et al. 2011). Computer algorithms assist in the photo ID of
104 species that have particularly fine-detailed patterning, and/or when dealing with large
105 databases (e.g. Andrzejczek et al. 2016; Germanov et al. 2019; Langley et al. 2020). Freely
106 available algorithms exist for a wide range of species, but the choice of algorithm can have
107 significant effects on the derived demographic parameter estimates. Misidentification of
108 matches can introduce false positives (i.e. two different individuals matched to the same ID)
109 and/or false negatives (i.e. one individual given two IDs). For example, a high false-
110 acceptance rate results in an under-estimation of population size, whereas a high false
111 rejection rate inflates estimates of population size (Hammond et al. 1990). The false-
112 acceptance rate can be reduced to effectively zero by visually confirming potential matches,
113 whereas the false-rejection rate is subject to multiple variables and so should be calculated
114 and reported per analysis (Hastings et al. 2001; Cunningham 2009).

115 Here we focus on three freely available pattern recognition software programmes:
116 ExtractCompare, I³S Pattern and Wild-ID. ExtractCompare was originally developed for grey
117 seals (Hiby and Lovell 1990) but has since been extended to other species (e.g. Eurasian
118 lynx *Lynx lynx*; Gimenez et al. 2019; Amur leopard *Panthera pardus orientalis*; Jiang et al.
119 2015; Vitkalova and Shevtsova 2016) and is currently the only pattern recognition software
120 which has a harbour seal specific model. The software builds a three-dimensional surface
121 model from reference points in a manually annotated image. Pattern cells are then extracted

122 from multiple aspects of the body (i.e. multibiometric identification; Jain 2007) to compare
123 the patterning on non-planar surfaces (Hiby and Lovell 1990). Pairs of images are ranked by
124 similarity scores and matches are manually confirmed. The software presents all potential
125 matches, but a similarity score threshold can be assigned to streamline the processing of
126 large datasets.

127 The Interactive Individual Identification System (I³S) has multiple versions designed to
128 extract and compare natural markings from a range of different species. I³S *Pattern* was
129 designed for species with hard to annotate markings such as lionfish (*Pterois volitans*;
130 Chaves et al. 2016) and turtles (Calmanovici et al. 2018). It employs a SURF (speeded-up
131 robust features) detector and descriptor, which first detects point correspondences between
132 images, then describes the area of interest and detects matches between these areas (Bay
133 et al. 2008). This is robust to noise, and variation in image scale and orientation, whilst
134 computing faster than pre-existing alternatives (such as the SIFT operator described below).
135 Similar to ExtractCompare, images are manually annotated with morphological reference
136 points and an extractable area, although these are specified by the user at data entry, along
137 with the number of potential matches presented.

138 Wild-ID was specifically designed to assist in the processing of large datasets generated by
139 monitoring populations using camera traps. The software employs a SIFT (scale-invariant
140 feature transform) operator which extracts distinctive image features whilst accounting for
141 image scale and rotation (Lowe 2004). The images are cropped prior to data entry as the
142 software does not distinguish the pattern of the subject from the pattern in the background
143 (i.e. the noise; Bolger et al. 2012). The software pattern comparison function is not species-
144 specific which enables its usability across a wide range of taxa, from amphibians (Bendik et
145 al. 2013; Mettouris et al. 2016; Pereira and Maneyro 2016) to mammals (Bolger et al. 2012;
146 Halloran et al. 2015). The standard version of the software then presents the top 20 potential
147 matches which require visual confirmation or rejection (Bolger et al. 2012).

148 The aim of this study was to test the performance of these three freely available pattern
149 recognition software programmes for the individual recognition of northeast Atlantic harbour
150 seals (*P. v. vitulina*). Photo ID data were collected as part of an ongoing project investigating
151 the regional decline in harbour seal numbers around Scotland (Arso Civil et al. 2016). Here,
152 software performance was measured as its ability to successfully score matching images
153 higher than non-matching images (Matthé et al. 2017). We investigated the effect of the data
154 collection methods and the aspect of the body from which the pattern cell was compared.
155 Data processing time was also compared between the three software programmes.

156

157 **Methods**

158 *Data collection*

159 Photo ID data were collected from harbour seal haulout sites in Kintyre, the Isle of Skye and
160 Orkney (Scotland), during the breeding seasons (June and July) of 2016, 2017 and 2018. In
161 Kintyre and Orkney, data were collected during dedicated land-based surveys from cliff tops
162 and beaches, 50-150m from harbour seal haulout sites, using a digiscope system
163 comprising of a DSLR camera attached to a scope (Swarovski ATS 80 with x20-60 eyepiece
164 and TLS-APO 30mm). On the Isle of Skye, data were collected from small tourist boats that
165 circumnavigate skerries where harbour seals haul out, 5-10m away from the boats, using a
166 DSLR camera with an 80-400mm zoom lens.

167 Photographs were graded for quality on a scale of 1 (poor) to 4 (excellent), following a
168 protocol adapted from Cunningham (2009), based on the focus of the image, the angle of
169 the seal to the photographer and the clarity of the pelage markings (i.e. lighting, wet/dry,
170 moult). Only images assigned a quality ≥ 3 were used in this analysis. Matches between
171 pairs of images were initially found manually and confirmed by a trained expert. A catalogue
172 of individual harbour seals with uniquely identifiable IDs was built and used to generate
173 databases to test the performance of each software.

174 *Database construction*

175 Multiple databases consisting of pairs of images from individual harbour seals were
176 constructed based on how the data were collected (scope, lens) and which aspect of the
177 body the pattern cell was extracted from (front head, left head, left neck, left flank; Fig. 1).
178 We excluded images from the right-hand side of the body as the algorithms should perform
179 as well with these as the left. We ensured that each image from a single individual were
180 collected on different sampling days, which avoided the likelihood of the backgrounds
181 matching (seals return to the water on each tide). Front head aspects were images of seals
182 facing the camera lens and included both eyes; left head aspects included the full side of the
183 head including the nose, eye and ear; left neck aspects included the area between the ear
184 and the fore-flipper; and left flank aspects included the area between the fore-flipper and the
185 pelvis. Flank aspects were not available from the Isle of Skye data as the photographer was
186 often too close to the seal to capture the entire body with a lens. Databases included pairs of
187 images from all available individuals for each data collection method and aspect; this ranged
188 from 65 to 178 individuals.

189 *Data processing*

190 We tested the performance of pattern recognition algorithms in detecting the one matching
191 image in a set of non-matching images. In order to standardise the methodology across
192 software (each has slightly different processing methods), data were entered in two batches
193 and only the images with the top 20 similarity scores were manually inspected. Manual
194 inspection in our study was of the image names which included the individual ID, but in a
195 real-world scenario this would be manual inspection of the pelage. Batch 1 was entered first,
196 containing a single image of each individual in that database. Batch 2 contained a second
197 different image of each individual and was then entered systematically and compared to
198 batch 1 (i.e. the library). Each database ($n = 7$) was run through each of the three software,
199 except for databases containing front heads (front head aspects cannot be processed in the
200 current ExtractCompare harbour seal model); this resulted in 19 trials. The process was
201 timed for each trial, from the first stage of data preparation through to the final stage of
202 match confirmation.

203 i) ExtractCompare

204 For ExtractCompare, images were reduced in size (i.e. cropped) prior to entry into the
205 Microsoft Access database as in the authors experience, this speeds up the processing time.
206 This software uses multibiometric identification and the pattern can be extracted from up to
207 five aspects of the body. However, this is subject to data availability, and chest and
208 abdomen aspects were underrepresented in our data. For this analysis, we focussed on left
209 heads, necks, and flanks. The left head aspect covers an area behind the eye which
210 includes the ear (Fig. 1a); the left neck aspect is the area between the ear and the fore
211 flipper (Fig. 1b); and the left flank aspect is the area between the fore flipper and the pelvis

212 (Fig. 1c). Images were annotated with the outline of the body and morphological reference
213 points which are specific to each aspect in question, but include the base of the skull, chin,
214 nose, eyes, ears, post-orbital vibrissae, flippers, and pelvis (Fig. 1).

215 ii) I³S Pattern

216 Cropping of images was not required for I³S pattern, and as far as possible, reference points
217 and extractable areas were specified so as to be as comparable across software as
218 possible. For front head aspects, the reference points identified were the right eye, the left
219 eye, and the nose, with the general identification area being a polygon from the eyes to the
220 top of the head (Fig. 1d). Left head aspects were identified by the nose, the left eye and the
221 left ear, and the area extended from the corner of the mouth to the back of the skull (Fig. 1e).
222 Left neck aspects were identified by the nose, the post-orbital vibrissae, and the fore flipper,
223 with the area extending from the corner of the mouth to the fore flipper (Fig. 1f). Finally, left
224 flank aspects were identified by the nose, the fore flipper, and the pelvis, with the identifiable
225 area extending from the fore flipper to the pelvis (Fig. 1g).

226 iii) Wild-ID

227 Wild-ID differs from the other two software programmes in that the pattern is not extracted
228 from an aspect of the subject but is compared across the entire image. Images were
229 therefore cropped to include only the desired aspect of the subject with as little of the
230 background noise as possible. To make the analysis comparable across the three software
231 programmes, we cropped images to the same aspects as with ExtractCompare and I³S
232 Pattern: front head (Fig. 1h), left head (Fig. 1i), left neck (Fig. 1j) and left flank (Fig. 1k).

233 *Performance analysis*

234 The pattern recognition software programmes used in this analysis are described as semi-
235 automated, as all require a final manual confirmation stage where the user has to accept or
236 reject each potential match. This reduces the overall likelihood of false acceptance (Sacchi
237 et al. 2016). For the purpose of this study, we focused on the recognition rate, defined as the
238 ability of the algorithm to successfully score matching images higher than non-matching
239 images (Matthé et al. 2017). The image filenames (which included the individual ID) of the
240 top 20 ranked similarity scores were visually inspected for each trial to manually confirm or
241 reject the potential match. The cumulative density function (CDF) was calculated for each
242 rank by dividing the cumulative sum of matches found by the number of matches available,
243 and the corresponding two-sided 95% confidence intervals (based on the binomial
244 distribution) were estimated using the *binom.test* function in R (R Core Team 2019). For a
245 software to perform well, the CDF should reach 1 within the fewest ranks possible; i.e. if the
246 match is not ranked high enough, the user could miss this (depending on any assigned
247 similarity score threshold) and the false-rejection rate would increase. More generally, the
248 lower down the potential matches a true match is ranked, the more time is required for the
249 user to find the match.

250 ExtractCompare, I³S Pattern and Wild-ID differ in data processing methodology and so
251 processing was timed for all trials. The different stages were made up of both manual and
252 automated steps. To run an image through ExtractCompare, there are five distinct stages:
253 cropping, data input, pattern extraction, batch comparison and visual confirmation. In I³S
254 Pattern, the stages of data input (pattern extraction, comparison, and confirmation) are
255 combined into a single step (combining manual and automated stages), and in Wild-ID, there
256 are four distinct stages: cropping, input/extraction, comparison and confirmation. Each stage

257 from data pre-processing to visual confirmation was timed separately and divided by the
258 number of images to give the time in minutes and seconds required to process a single
259 image (data processing rate).

260

261 **Results**

262 Across each tested scenario, Wild-ID outperformed both ExtractCompare and I³S Pattern for
263 harbour seal pattern recognition (Table 1, Fig 2). This trend was most pronounced when
264 comparing the pelage pattern from the left head (CDF = 0.49-0.66) and neck regions (CDF =
265 0.45-0.64), regardless of data collection method, and for front head aspects taken using a
266 camera and lens (CDF = 0.58-0.71). Data collected using a camera and lens had a higher
267 proportion of the highest quality images (lens=0.62, scope=0.27) and in general, the highest
268 performance for each software came from using data collected with a camera and lens (Fig.
269 2).

270 In Wild-ID, front head aspects performed highest; when only visually inspecting the top
271 ranked potential match, the CDF was 0.58, translating to a false-rejection rate (FRR; 1-CDF)
272 of 0.42. When the top 20 ranked potential matches were visually inspected, the CDF
273 reached the highest recorded in this study: 0.71 (with an associated FRR of 0.29).
274 Conversely, ExtractCompare performed best with left head aspects (CDF₁=0.36 with a FRR
275 of 0.64; CDF₂₀=0.55 with a FRR of 0.45). Indeed, by rank 10, the uncertainty around the
276 CDF for ExtractCompare overlapped with that of Wild-ID. I³S Pattern performed poorly in
277 most scenarios except for in trials which used front head aspects. As with Wild-ID, the
278 highest CDF₁ for I³S Pattern was recorded from front head aspects taken using a camera
279 and lens (CDF₁=0.30 with a FRR of 0.70). The performance of front head aspects taken
280 using a camera and scope however was much more comparable to that of Wild-ID.

281 With all processing stages combined, Wild-ID had the highest data processing rate (i.e. the
282 least amount of time per image processed; mean ± sd mm:ss, 00:22 ± 00:04), followed by
283 I³S Pattern (00:31 ± 00:04) and ExtractCompare (01:36 ± 00:08; Table 2). For
284 ExtractCompare, the vast proportion of time was spent in the pattern extraction stage (01:01
285 ± 00:06; 64% of total time) where images were annotated, and the three-dimensional model
286 was applied. The remaining time was spread across cropping (00:09 ± 00:04; 9%), input
287 (00:08 ± 00:02; 8%), comparison (00:05 ± 00:01; 5%) and confirmation stages (00:12 ±
288 00:02; 13%). The data processing in I³S Pattern was shorter than ExtractCompare and
289 cropping was not required prior to data entry. For Wild-ID, images were cropped prior to
290 entry which took the greatest proportion of time (00:16 ± 00:04; 73%). Data input and pattern
291 extraction stages were combined into one (<00:01 ± <00:01; 4%) and were followed by short
292 comparison (00:01 ± <00:01; 5%) and confirmation stages (00:04 ± 00:01; 18%).

293

294 **Discussion**

295 The highest performing pattern recognition software tested for harbour seal photo ID was
296 Wild-ID, followed by ExtractCompare and then I³S Pattern. The strength of this trend varied
297 with the data collection method and the aspect of the body that the pattern was compared
298 from. Importantly, Wild-ID also required the least amount of time to run a single image
299 through the stages from pre-processing to match confirmation. The highest recorded CDF,
300 and therefore the lowest FRR, was recorded in Wild-ID for front head aspects collected

301 using a camera and lens ($CDF_{20}=0.71$; $FRR=0.29$). This error is within a range deemed
302 acceptable for the estimation of population parameters (Hiby et al. 2013).

303 In the present study, photo ID data were either collected from a platform 50-150m away from
304 the seal (using a digiscope) or from a boat within 10m of the seal (using a lens). The data
305 collection method was therefore used as a proxy for distance to haulout, which has been
306 shown to influence image quality (Bendik et al. 2013). In this study, within each aspect, data
307 collected using a lens performed marginally better than data collected using a scope.
308 Previous photo ID studies have found that image quality has influenced the performance of
309 pattern recognition algorithms. In ExtractCompare for harbour seals, the false-rejection rate
310 has been shown to decrease from 73% to 2% by increasing image quality alone (Hastings et
311 al. 2008). Similar trends have been reported for I³S Pattern (Steinmetz et al. 2018) and Wild-
312 ID (Bendik et al. 2013). Halloran et al. (2015) investigated the effect of image quality further
313 and found that the only variable which affected the ability of Wild-ID to detect matches
314 between images of Thornicroft's giraffe (*Giraffa camelopardalis thornicrofti*) was background
315 complexity. This effect could therefore be reduced by cropping the images or by digitally
316 removing the background entirely (Bolger et al. 2012; Chehrsimin et al. 2018).

317 The patterned surface of a seal's pelage is non-planar and can appear very different
318 depending on the animal's orientation and torsion (Hiby and Lovell 1990). This is most
319 pronounced on regions such as the neck and flank, whereas the region around the head is
320 less susceptible to this distortion. Additionally, repeatability in the manual placement of the
321 pattern cell is easier in the head region due to the proximity of obvious morphological
322 features (i.e. eyes, ears, nose). In this study, ExtractCompare performed best with left head
323 aspects. In previous studies, ExtractCompare has been shown to perform well for harbour
324 seals using the shoulder/neck regions (Cunningham 2009) and ventral aspects (Hastings et
325 al. 2008). The neck aspect is a larger region than the head and so contains more of an
326 individual's unique "fingerprint", but it is also possibly more difficult to standardise across
327 images. Ventral aspects were underrepresented in our dataset given the haulout behaviour
328 of seals at the sites in this study, although it would be interesting to explore whether the
329 performance of ExtractCompare, along with I³S Pattern and Wild-ID, could be improved for
330 northeast Atlantic harbour seal photo ID if images of the ventral side of the animals could be
331 collected.

332 Conversely, we found that both Wild-ID and I³S Pattern performed best for harbour seal
333 photo ID using front head aspects. Previous studies have found I³S Pattern to perform highly
334 in the photo ID of green turtles (*Chelonia mydas*; Den Hartog and Reijns 2014), Hawksbill
335 turtles (*Eretmochelys imbricate*; Steinmetz et al. 2018) and *Tarentola* geckos (Rocha et al.
336 2013); the natural patterning of all are found on rigid body parts (e.g. carapace scutes). The
337 fore-head region of a harbour seal is also relatively rigid, and so best satisfies the
338 assumption within I³S Pattern that animals have linearity (i.e. their body parts do not move in
339 respect to one another; Den Hartog and Reijns 2014).

340 When choosing a pattern recognition software to assist in the analysis of photo ID data, the
341 ability of the software to detect a match is important, but often the amount of time required to
342 process data is also crucial. Pattern matching algorithms have dramatically reduced the
343 number of images which need to be visually inspected to find a match (Hastings et al. 2001;
344 Morrison et al. 2011). This is important for long-term population studies that rely on detecting
345 matches between thousands of images which would not be feasible though manual
346 matching alone. In this study, the time required to process a single image using Wild-ID was

347 on average 22s, compared with 31s in I³S Pattern and 1m36s in ExtractCompare; the
348 processing time of images in ExtractCompare was >4x greater than in Wild-ID. However, it is
349 important to note that data processing included both manual and automated stages, and
350 time can be saved by running automated stages overnight or alongside other tasks.

351 We tested the ability of the software algorithms to not only detect a positive match but also to
352 rank it higher than non-matching images. The time required to manually inspect each
353 potential match can be substantial and so often thresholds are assigned, below which
354 potential matches are rejected without inspection. In ExtractCompare, previous studies have
355 assigned thresholds on similarity scores of 0.95 (Hiby et al. 2013) and 0.75 (Langley et al.
356 2020) for grey seal photo ID, and 0.45 for cheetah photo ID (Kelly 2001). In I³S Pattern, it
357 has been more common to assign a threshold on the number of potential matches that are
358 visually inspected (e.g. 50; Rocha et al. 2013; Steinmetz et al. 2018). Previous studies which
359 use Wild-ID have also assigned thresholds on the similarity scores generated, and for
360 species that can be easily manipulated, cleaned and posed against white backgrounds (e.g.
361 Amphibians; Bardier et al. 2017), similarity scores are consistently predictive of positive
362 matches (Bendik et al. 2013). However, with other taxa there is evidence that the similarity
363 scores in Wild-ID can be affected by allometric variation; i.e. when individuals are still
364 growing (Bardier et al. 2017), and in these cases the time between photographs can reduce
365 similarity scores (Bendik et al. 2013). In this study our data were limited to adult harbour
366 seals, but it would be useful to test the performance of pattern recognition software in
367 detecting matches between pups, juveniles and adults; as has been successful using
368 ExtractCompare for grey seals (Paterson et al. 2013).

369 Setting thresholds for manual review can significantly increase the efficiency of data
370 processing but comes with associated false-rejection rates (Hiby et al. 2013). These errors
371 are not consistent across studies and/or sub-species, with previous harbour seal photo ID
372 analyses using ExtractCompare reporting error rates of 6.2% (Hastings et al. 2001) and
373 21.4% (McCormack 2015). False-rejection rates for I³S Pattern and Wild-ID are not available
374 for harbour seals but are low for the species that the algorithms were initially designed for.
375 For example, the false rejection rate (using only the top ranked potential match) for the photo
376 ID of green turtles (*Chelonia mydas*) in I³S Pattern was 14% (Den Hartog and Reijns 2014),
377 and for Masai giraffe (*Giraffa camelopardalis tippelskirchi*) photo ID in Wild-ID was 0.7%
378 (Bolger et al. 2012). False-rejection rates are therefore variable and can be influenced by the
379 experience of software users (Bolger et al. 2012) and the number of images from the same
380 individuals (Hiby et al. 2013); along with variables tested in this study.

381 In this study we compared the performance of three freely available software, but there are
382 additional software algorithms available; these include, but are not limited to, ICEIS/
383 Hotspotter (Crall et al. 2013), Discovery (Gailey and Karczmarski 2012) and StripeSpotter
384 (Lahiri et al. 2011). Investigation into the performance of other software algorithms for
385 harbour seal photo ID, and their comparison to Wild-ID, would be a valuable next step.
386 Beyond that, as ecological research becomes increasingly data-heavy, methods such as
387 photo ID lend themselves to automation. Existing photo ID databases are required to train
388 algorithms to automatically locate a seal within an image (i.e. segmentation; Chehrsimin et
389 al. 2018), extract pelage pattern, describe this pattern and then compare it to a library of
390 known individuals. As it stands, artificial intelligence for pattern recognition requires manually
391 annotated databases. There is also a strong argument for manual confirmation of detected
392 matches, at least until the error rates are below an accepted threshold. However, at the very

393 least, automating the data pre-processing and input stages will help to improve the efficiency
394 of pattern recognition software further.

395

396 **Compliance with ethical standards**

397 This research was approved by the University of St Andrews Animal Welfare and Ethics
398 Committee (AWEC) and data collection was funded by the Scottish Government (grant
399 number MMSS/002/15). The authors declare that they have no conflicts of interest.

400

401 **Author contributions**

402 IL & MAC conceived and designed the analysis, IL, EH & MAC collected the data, IL
403 performed the analysis and wrote the paper, and EH & MAC read and commented on
404 multiple drafts.

405

406 **References**

407 Andrzejaczek S, Meeuwig J, Rowat D, Pierce S, Davies T, Fisher R, Meekan M (2016) The
408 ecological connectivity of whale shark aggregations in the Indian Ocean: a photo-
409 identification approach. *Royal Society Open Science* 3(11):160455.
410 <https://doi.org/10.1098/rsos.160455>

411 Arso Civil M, Smout S, Onoufriou J, Thompson D, Brownlow A, Davison N, Cummings C,
412 Pomeroy P, McConnell B, Hall A (2016) Harbour Seal Decline - vital rates and drivers
413 (Report to Scottish Government HSD2). Retrieved from Sea Mammal Research Unit,
414 University of St Andrews: [http://www.smru.st-andrews.ac.uk/files/2016/10/HSD-2-annual-
415 report-year-1.pdf](http://www.smru.st-andrews.ac.uk/files/2016/10/HSD-2-annual-report-year-1.pdf)

416 Arzoumanian Z, Holmberg J, Norman B (2005) An astronomical pattern-matching algorithm
417 for computer-aided identification of whale sharks *Rhincodon typus*. *Journal of Applied*
418 *Ecology* 42(6):999-1011. <https://doi.org/10.1111/j.1365-2664.2005.01117.x>

419 Bay H, Ess A, Tuytelaars T, Van Gool L (2008) Speeded-up robust features (SURF).
420 *Computer Vision and Image Understanding* 110(3):346-359.
421 <https://doi.org/10.1016/j.cviu.2007.09.014>

422 Bendik NF, Morrison TA, Gluesenkamp AG, Sanders MS, O'Donnell LJ (2013) Computer-
423 assisted photo identification outperforms visible implant elastomers in an endangered
424 salamander, *Eurycea tonkawae*. *PloS one* 8(3):e59424.
425 <https://doi.org/10.1371/journal.pone.0059424>

426 Bolger DT, Morrison TA, Vance B, Lee D, Farid H (2012) A computer-assisted system for
427 photographic mark-recapture analysis. *Methods in Ecology and Evolution* 3(5):813-822.
428 <https://doi.org/10.1111/j.2041-210X.2012.00212.x>

429 Bradshaw CJ, Mollet HF, Meekan MG (2007) Inferring population trends for the world's
430 largest fish from mark-recapture estimates of survival. *Journal of Animal Ecology*
431 76(3):480-489. <https://doi.org/10.1111/j.1365-2656.2006.01201.x>

- 432 Button CA, Rogers-Bennett L (2011) Vital rates of pink abalone *Haliotis corrugata* estimated
433 from mark-recapture data to inform recovery. Marine Ecology Progress Series 431:151-
434 161. <https://doi.org/10.3354/meps09094>
- 435 Caiafa CF, Proto AN, Vergani D, Stanganelli Z (2005) Development of individual recognition
436 of female southern elephant seals, *Mirounga leonina*, from Punta Norte Península
437 Valdés, applying principal components analysis. Journal of Biogeography 32(7):1257-
438 1266. <https://doi.org/10.1111/j.1365-2699.2004.01215.x>
- 439 Calmanovici B, Waayers D, Reisser J, Clifton J, Proietti M (2018) I³S Pattern as a mark-
440 recapture tool to identify captured and free-swimming sea turtles: an assessment. Marine
441 Ecology Progress Series 589:263-8. <https://doi.org/10.3354/meps12483>
- 442 Chaves LCT, Hall J, Feitosa JLL, Côté IM (2016) Photo-identification as a simple tool for
443 studying invasive lionfish *Pterois volitans* populations. Journal of Fish Biology 88(2):800-
444 804. <https://doi.org/10.1111/jfb.12857>
- 445 Chehrsimin T, Eerola T, Koivuniemi M, Auttila M, Levänen R, Niemi M, Kunnasranta M,
446 Kälviäinen H (2018) Automatic individual identification of Saimaa ringed seals. IET
447 Computer Vision 12(2):146-152. <https://doi.org/10.1049/iet-cvi.2017.0082>
- 448 Crall JP, Stewart CV, Berger-Wolf TY, Rubenstein DI, Sundaresan SR (2013) Hotspotter –
449 Patterned species instance recognition. IEEE workshop on applications of computer
450 vision (WACV) 230-237. <https://doi.org/10.1109/WACV.2013.6475023>
- 451 Cunningham L (2009) Using computer-assisted photo-identification and capture-recapture
452 techniques to monitor the conservation status of harbour seals (*Phoca vitulina*). Aquatic
453 Mammals 35(3):319-329. <https://doi.org/10.1578/AM.35.3.2009.319>
- 454 Den Hartog J, Reijns R (2014) I³S Pattern Manual. Interactive Individual Identification
455 System. Version 4.0.2. <http://www.reijns.com/i3s/download/I3S%20Pattern.pdf>. Accessed
456 25th September 2020
- 457 Gailey G, Karczmarski L (2012) Discovery: Photo-identification data-management system for
458 individually recognizable animals. Available from:
459 <http://www.biosch.hku.hk/ecology/staffhp/lk/Discovery/>
- 460 Germanov ES, Bejder L, Chabanne DB, Dharmadi D, Hendrawan IG, Marshall AD, Pierce
461 SJ, van Keulen M, Loneragan NR (2019) Contrasting habitat use and population
462 dynamics of reef manta rays within the Nusa Penida Marine Protected Area, Indonesia.
463 Frontiers in Marine Science 6(215). <https://doi.org/10.3389/fmars.2019.00215>
- 464 Gimenez O, Gatti S, Duchamp C, Germain E, Laurent A, Zimmermann F, Marboutin E
465 (2019) Spatial density estimates of Eurasian lynx (*Lynx lynx*) in the French Jura and
466 Vosges Mountains. Ecology and Evolution 9(20):11707-11715.
467 <https://doi.org/10.1002/ece3.5668>
- 468 Gore MA, Frey PH, Ormond RF, Allan H, Gilkes G (2016) Use of photo-identification and
469 mark-recapture methodology to assess basking shark (*Cetorhinus maximus*) populations.
470 PLoS One 11(3):e0150160. <https://doi.org/10.1371/journal.pone.0150160>
- 471 Goswami VR, Madhusudan MD, Karanth KU (2007) Application of photographic capture-
472 recapture modelling to estimate demographic parameters for male Asian elephants.
473 Animal Conservation 10(3):391-399. <https://doi.org/10.1111/j.1469-1795.2007.00124.x>

474 Halloran KM, Murdoch JD, Becker MS (2015) Applying computer-aided photo-identification
475 to messy datasets: a case study of Thornicroft's giraffe (*Giraffa camelopardalis*
476 *thornicrofti*). *African Journal of Ecology* 53(2):147-155. <https://doi.org/10.1111/aje.12145>

477 Hammond PS, Mizroch SA, Donovan GP (1990) Individual recognition of cetaceans: Use of
478 photo-identification and other techniques to estimate population parameters. Report of
479 the International Whaling Commission 12.

480 Hastings KK, Small RJ, Hiby L (2001) Use of computer-assisted matching of photographs to
481 examine population parameters of Alaskan harbor seals. In: Harbor Seal Investigations in
482 Alaska. Annual Report for NOAA Award NA87FX0300. Alaska Department of Fish and
483 Game, Division of Wildlife Conservation, Anchorage, AK, 146-160.

484 Hastings KK, Hiby LA, Small RJ (2008) Evaluation of a computer-assisted photograph-
485 matching system to monitor naturally marked harbor seals at Tugidak Island, Alaska.
486 *Journal of Mammalogy* 89(5):1201-1211. <https://doi.org/10.1644/07-MAMM-A-151.1>

487 Hiby L, Lovell P (1990) Computer aided matching of natural markings: a prototype system
488 for grey seals. Report of the International Whaling Commission 12:57-61.

489 Hiby L, Lundberg T, Karlsson O, Watkins J, Jüssi M, Jüssi I, Helander B (2007) Estimates of
490 the size of the Baltic grey seal population based on photo-identification data. NAMMCO
491 scientific publications 6:163-175. <https://doi.org/10.7557/3.2731>

492 Hiby L, Paterson WD, Redman P, Watkins J, Twiss SD, Pomeroy P (2013) Analysis of
493 photo-id data allowing for missed matches and individuals identified from opposite sides.
494 *Methods in Ecology and Evolution* 4(3):252-9. <https://doi.org/10.1111/2041-210x.12008>

495 Jain AK (2007) Biometric recognition. *Nature* 449(7158):38-40.
496 <https://doi.org/10.1038/449038a>

497 Jiang G, Qi J, Wang G, Shi Q, Darman Y, Hebblewhite M, Miquelle DG, Li Z, Zhang X, Gu J,
498 Chang Y (2015) New hope for the survival of the Amur leopard in China. *Scientific*
499 *Reports* 5:15475. <https://doi.org/10.1038/srep15475>

500 Kelly BP (1981) Pelage polymorphism in Pacific harbor seals. *Canadian Journal of Zoology*
501 59(7):1212-1219. <https://doi.org/10.1139/z81-173>

502 Kelly MJ (2001) Computer-aided photograph matching in studies using individual
503 identification: an example from Serengeti cheetahs. *Journal of Mammalogy* 82:440-449.
504 [https://doi.org/10.1644/1545-1542\(2001\)082<0440:CAPMIS>2.0.CO;2](https://doi.org/10.1644/1545-1542(2001)082<0440:CAPMIS>2.0.CO;2)

505 Koivuniemi M, Auttila M, Niemi M, Levänen R, Kunnasranta M (2016) Photo-ID as a tool for
506 studying and monitoring the endangered Saimaa ringed seal. *Endangered Species*
507 *Research* 30:29-36. <https://doi.org/10.3354/esr00723>

508 Lahiri M, Tantipathananandh C, Warungu R, Rubenstein DI, Berger-Wolf TY (2011)
509 Biometric animal databases from field photographs: Identification of individual zebra in
510 the wild. *Proceedings of the ACM International Conference on Multimedia Retrieval*
511 (ICMR) 1-8. <https://doi.org/10.1145/1991996.1992002>

512 Langley I, Rosas Da Costa Oliver TV, Hiby L, Stringell T, Morris C, O'Cahtla O, Morgan L,
513 Lock K, Perry S, Westcott S, Boyle D, Büche BI, Stubbings EM, Boys RM, Self H,
514 Lindenbaum C, Strong P, Baines M, Pomeroy PP (2020) Site use and connectivity of

515 female grey seals (*Halichoerus grypus*) around Wales. Marine Biology 167:86.
516 <https://doi.org/10.1007/s00227-020-03697-8>

517 Letcher BH, Schueller P, Bassar RD, Nislow KH, Coombs JA, Sakrejda K, Morrissey M,
518 Sigourney DB, Whiteley AR, O'Donnell MJ, Dubreuil TL (2015) Robust estimates of
519 environmental effects on population vital rates: An integrated capture-recapture model of
520 seasonal brook trout growth, survival and movement in a stream network. Journal of
521 Animal Ecology 84(2):337-352. <https://doi.org/10.1111/1365-2656.12308>

522 Lowe DG (2004) Distinctive image features from scale-invariant keypoints. International
523 Journal of Computer Vision 60(2):91-110.
524 <https://doi.org/10.1023/B:VISI.0000029664.99615.94>

525 Mackey BL, Durban JW, Middlemas SJ, Thompson PM (2008) A Bayesian estimate of
526 harbour seal survival using sparse photo-identification data. Journal of Zoology
527 274(1):18-27. <https://doi.org/10.1111/j.1469-7998.2007.00352.x>

528 Matthé M, Sannolo M, Winiarski K, Spitzen-van der Sluijs A, Goedbloed D, Steinfartz S,
529 Stachow U (2017) Comparison of photo-matching algorithms commonly used for
530 photographic capture-recapture studies. Ecology and Evolution 7(15):5861-5872.
531 <https://doi.org/10.1002/ece3.3140>

532 McCormack M (2015) Assessing the applicability of computer aided photo-identification for
533 Pinniped studies through the determination of site fidelity in Long Island, NY harbor seals
534 (*Phoca vitulina concolor*). Dissertation, University of Miami.

535 Mettouris O, Megremis G, Giokas S (2016) A newt does not change its spots: using pattern
536 mapping for the identification of individuals in large populations of newt species.
537 Ecological Research 31(3):483-489. <https://doi.org/10.1007/s11284-016-1346-y>

538 Morrison TA, Yoshizaki J, Nichols JD, Bolger DT (2011) Estimating survival in photographic
539 capture-recapture studies: Overcoming misidentification error. Methods in Ecology and
540 Evolution 2(5):454-463. <https://doi.org/10.1111/j.2041-210X.2011.00106.x>

541 Morton AC (1982) The effects of marking and capture on recapture frequencies of butterflies.
542 Oecologia 53(1):105-110. <https://doi.org/10.1007/BF00377143>

543 Paterson WD, Redman P, Hiby LA, Moss SE, Hall AJ, Pomeroy P (2013) Pup to adult
544 photo-ID: Evidence of pelage stability in gray seals. Marine Mammal Science 29(4):537-
545 541. <https://doi.org/10.1111/mms.12043>

546 Pereira G, Maneyro R (2016) Movement patterns in a Uruguayan population of
547 *Melanophryniscus montevidensis* (Philippi, 1902) (Anura: Bufonidae) using photo-
548 identification for individual recognition. South American Journal of Herpetology 11(2):119-
549 126. <https://doi.org/10.2994/SAJH-D-15-00020.1>

550 R Core Team (2019) R: A language and environment for statistical computing. R Foundation
551 for Statistical Computing, Vienna, Austria. <https://www.R-project.org/>

552 Rocha R, Carrilho T, Rebelo R (2013) Iris photo-identification: A new methodology for the
553 individual recognition of Tarentola geckos. Amphibia-Reptilia 34:590-596.
554 <https://doi.org/10.1163/15685381-00002918>

555 Rotella JJ, Link WA, Chambert T, Stauffer GE, Garrott RA (2012) Evaluating the
556 demographic buffering hypothesis with vital rates estimated for Weddell seals from 30

557 years of mark–recapture data. *Journal of Animal Ecology* 81(1):162-173.
558 <https://doi.org/10.1111/j.1365-2656.2011.01902.x>

559 Sacchi R, Scali S, Mangiacotti M, Sannolo M, Zuffi MA (2016) Digital identification and
560 analysis. In: Dodd CK (ed) *Reptile Ecology and Conservation A Handbook of Techniques*.
561 Oxford University Press, pp 59-72.

562 Sherwin RE, Haymond S, Stricklan D, Olsen R (2002) Freeze-branding to permanently mark
563 bats. *Wildlife Society Bulletin* 97-100. <https://www.jstor.org/stable/3784641>

564 Steinmetz K, Webster I, Rowat D, Bluemel JK (2018) Evaluating the Software I3S Pattern for
565 Photo-Identification of Nesting Hawksbill Turtles (*Eretmochelys imbricata*). *Marine Turtle*
566 *Newsletter* 155:15-19.

567 Thompson PM, Wheeler H (2008) Photo-ID-based estimates of reproductive patterns in
568 female harbor seals. *Marine Mammal Science* 24(1):138-146.
569 <https://doi.org/10.1111/j.1748-7692.2007.00179.x>

570 Vernes K, Freeman M, Nesbitt B (2009) Estimating the density of free-ranging wild horses in
571 rugged gorges using a photographic mark-recapture technique. *Wildlife Research*
572 36(5):361-367. <https://doi.org/10.1071/WR07126>

573 Vitkalova AV, Shevtsova EI (2016) A complex approach to study the Amur leopard using
574 camera traps in protected areas in the southwest of Primorsky Krai (Russian Far East).
575 *Nature Conservation Research Заповедная наука* 1(3).

576 Wells RS, Scott MD (1990) Estimating bottlenose dolphin population parameters from
577 individual identification and capture-release techniques. *Report of the International*
578 *Whaling Commission* 12:407-415.

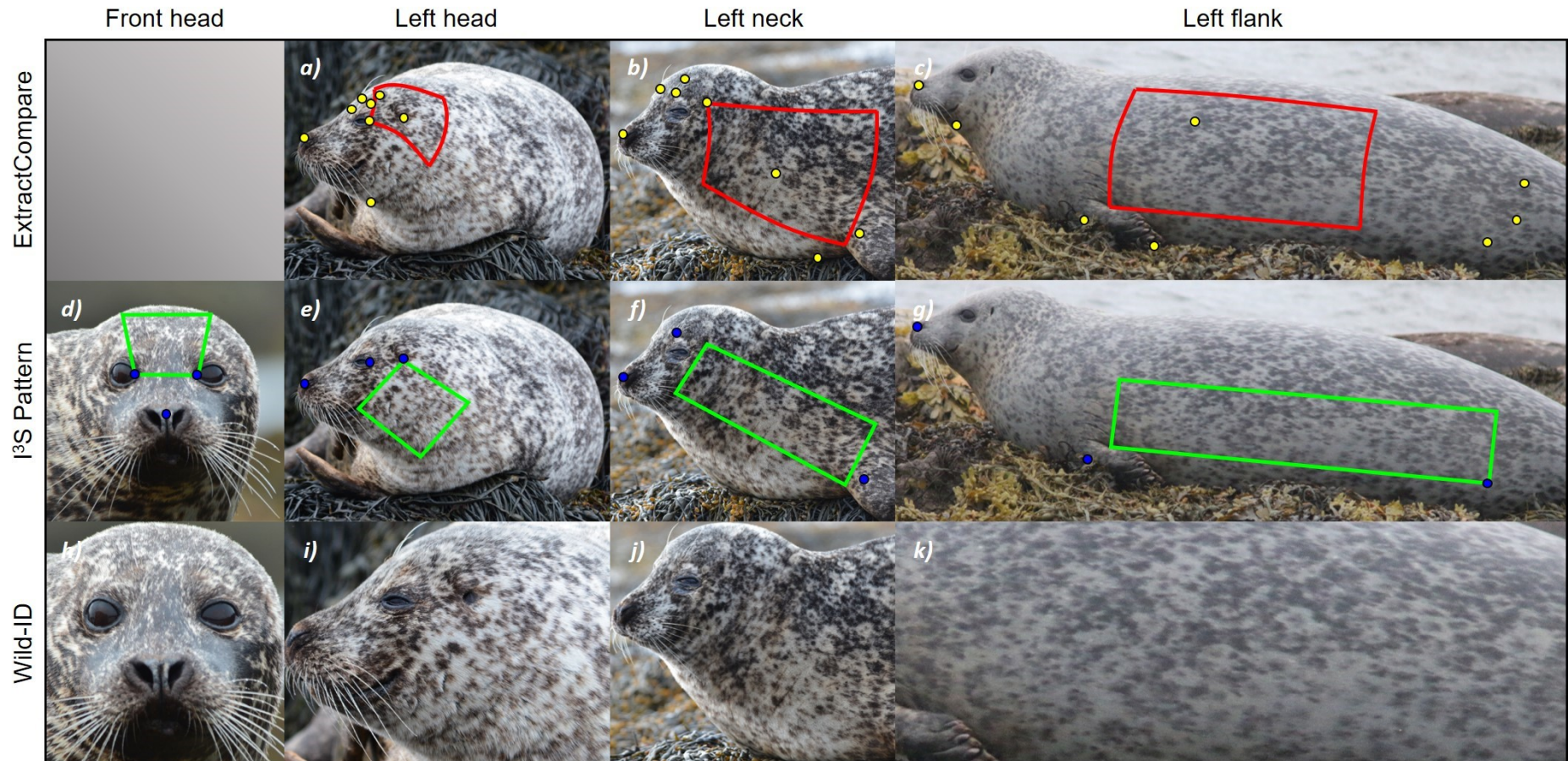
579 Yochem PK, Stewart BS, Mina M, Zorin A, Sadovov V, Yablokov A (1990) Non-metrical
580 analyses of pelage patterns in demographic studies of harbor seals. *Report of the*
581 *International Whaling Commission* 12:87-90.

582 Zimmerman GS, Gutierrez RJ, Lahaye WS (2007) Finite study areas and vital rates:
583 sampling effects on estimates of spotted owl survival and population trends. *Journal of*
584 *Applied Ecology* 44(5):963-971. <https://doi.org/10.1111/j.1365-2664.2007.01343.x>

585

586

587

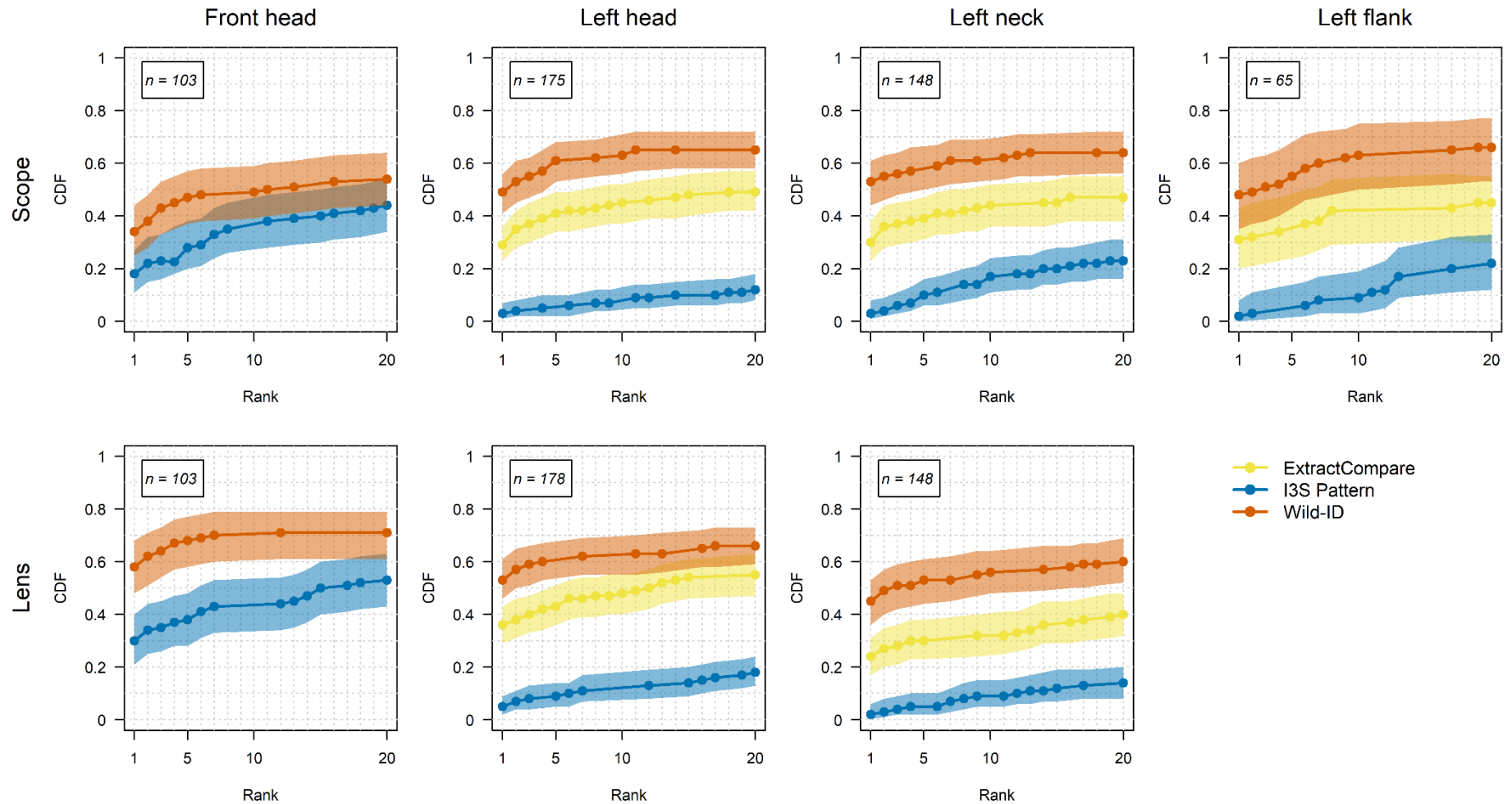


588

589 **Fig. 1** Aspect specific reference points and extractable areas used to compare the pelage pattern of harbour seals using ExtractCompare, I³S
 590 Pattern and Wild-ID. Top row (ExtractCompare): reference points (yellow dots) and extractable area (red box). Middle row (I³S Pattern):
 591 reference points (blue dots) and extractable area (green box). Bottom row (Wild-ID): Wild-ID does not use reference points and so the
 592 extractable area is the cropped aspect of the subject.

593

594



595

596 **Fig. 2** The cumulative density function (CDF) of the matches detected by ranked similarity score. Trials were run for each pattern recognition
 597 software: ExtractCompare (yellow), I³S Pattern (blue) and Wild-ID (red), by data collection equipment (scope, lens) and seal aspect (front head,
 598 left head, left neck, left flank). Shaded areas represent 95% confidence intervals based on the binomial distribution.

599 Table 1. The cumulative density function and 95% confidence intervals for potential matches ranked in first position (CDF₁), and within the top
600 5, 10 and 20 ranks (CDF₅, CDF₁₀, and CDF₂₀ respectively); *n* is the number of individuals in each database, Db (number of images = 2*n*). Flank
601 aspects were not available from the lens data (as often the photographer was too close to the seal to capture the entire body) and front head
602 aspects cannot be processed in the current ExtractCompare harbour seal model.

Trial	Db	Method	Aspect	<i>n</i>	Software	CDF ₁	CDF ₅	CDF ₁₀	CDF ₂₀
1	A	Scope	Front head	103	I ³ S Pattern	0.18 (0.11, 0.27)	0.28 (0.20, 0.38)	0.35 (0.26, 0.45)	0.44 (0.34, 0.54)
2	A	Scope	Front head	103	Wild-ID	0.34 (0.25, 0.44)	0.47 (0.37, 0.57)	0.49 (0.39, 0.59)	0.54 (0.44, 0.64)
3	B	Lens	Front head	103	I ³ S Pattern	0.30 (0.21, 0.40)	0.38 (0.28, 0.48)	0.43 (0.33, 0.53)	0.53 (0.43, 0.63)
4	B	Lens	Front head	103	Wild-ID	0.58 (0.48, 0.68)	0.68 (0.58, 0.77)	0.70 (0.60, 0.79)	0.71 (0.61, 0.79)
5	C	Scope	Left head	175	ExtractCompare	0.29 (0.23, 0.36)	0.41 (0.34, 0.49)	0.45 (0.37, 0.52)	0.49 (0.42, 0.57)
6	C	Scope	Left head	175	I ³ S Pattern	0.03 (0.01, 0.07)	0.05 (0.02, 0.10)	0.07 (0.04, 0.12)	0.12 (0.08, 0.18)
7	C	Scope	Left head	175	Wild-ID	0.49 (0.41, 0.56)	0.61 (0.53, 0.68)	0.63 (0.56, 0.71)	0.65 (0.58, 0.72)
8	D	Lens	Left head	178	ExtractCompare	0.36 (0.29, 0.43)	0.43 (0.36, 0.51)	0.48 (0.40, 0.55)	0.55 (0.47, 0.63)
9	D	Lens	Left head	178	I ³ S Pattern	0.05 (0.02, 0.09)	0.09 (0.05, 0.14)	0.11 (0.07, 0.17)	0.18 (0.13, 0.24)
10	D	Lens	Left head	178	Wild-ID	0.53 (0.46, 0.61)	0.60 (0.53, 0.67)	0.62 (0.55, 0.69)	0.66 (0.59, 0.73)
11	E	Scope	Left neck	148	ExtractCompare	0.30 (0.23, 0.38)	0.39 (0.31, 0.47)	0.44 (0.36, 0.52)	0.47 (0.38, 0.55)
12	E	Scope	Left neck	148	I ³ S Pattern	0.03 (0.01, 0.08)	0.10 (0.06, 0.16)	0.17 (0.11, 0.24)	0.23 (0.16, 0.31)
13	E	Scope	Left neck	148	Wild-ID	0.53 (0.44, 0.61)	0.57 (0.49, 0.66)	0.62 (0.54, 0.70)	0.64 (0.56, 0.72)
14	F	Lens	Left neck	148	ExtractCompare	0.24 (0.17, 0.31)	0.30 (0.23, 0.38)	0.32 (0.24, 0.40)	0.40 (0.32, 0.48)
15	F	Lens	Left neck	148	I ³ S Pattern	0.02 (0.004, 0.06)	0.05 (0.02, 0.10)	0.09 (0.05, 0.15)	0.14 (0.08, 0.20)
16	F	Lens	Left neck	148	Wild-ID	0.45 (0.36, 0.53)	0.53 (0.44, 0.61)	0.56 (0.48, 0.64)	0.60 (0.52, 0.69)
17	G	Scope	Left flank	65	ExtractCompare	0.31 (0.20, 0.43)	0.34 (0.23, 0.47)	0.42 (0.29, 0.54)	0.45 (0.30, 0.55)
18	G	Scope	Left flank	65	I ³ S Pattern	0.02 (0.0004, 0.08)	0.03 (0.004, 0.11)	0.09 (0.03, 0.19)	0.22 (0.12, 0.33)
19	G	Scope	Left flank	65	Wild-ID	0.48 (0.35, 0.60)	0.55 (0.43, 0.68)	0.63 (0.50, 0.75)	0.66 (0.53, 0.77)

603

604

605 Table 2. Data processing rate (time in minutes:seconds for a single image to be processed, from pre-processing to visual confirmation). Trials
606 correspond to Table 1; n is the number of individuals within each database (number of images = $2n$); timed stages were crop (image cropping),
607 input (data input), extract (pattern extract), compare (pattern comparison), and confirm (visual confirmation). In I³S Pattern, the stages from
608 data input to visual confirmation were combined into a single step, represented below by merged cells.

Software	Trial	Method	Aspect	n	Crop	Input	Extract	Compare	Confirm	Overall
ExtractCompare	5	Scope	Left head	175	00:10	00:07	00:53	00:05	00:10	01:25
	8	Lens	Left head	178	00:10	00:11	00:59	00:06	00:13	01:39
	11	Scope	Left neck	148	00:10	00:07	01:10	00:06	00:12	01:45
	14	Lens	Left neck	148	00:09	00:09	01:03	00:05	00:15	01:40
	17	Scope	Left flank	65	00:10	00:08	00:59	00:03	00:12	01:32
I ³ S Pattern	1	Scope	Front head	103	NA	00:33				00:33
	3	Lens	Front head	103	NA	00:31				00:31
	6	Scope	Left head	175	NA	00:35				00:35
	9	Lens	Left head	178	NA	00:31				00:31
	12	Scope	Left neck	148	NA	00:22				00:22
	15	Lens	Left neck	148	NA	00:31				00:31
Wild-ID	2	Scope	Front head	103	00:16	<00:01	00:01	00:06	<00:01	00:22
	4	Lens	Front head	103	00:15	<00:01	00:01	00:03	<00:01	00:19
	7	Scope	Left head	175	00:14	<00:01	00:01	00:04	<00:01	00:20
	10	Lens	Left head	178	00:14	00:01	00:01	00:06	00:01	00:21
	13	Scope	Left neck	148	00:15	00:01	00:01	00:05	00:01	00:22
	16	Lens	Left neck	148	00:14	00:01	00:02	00:05	00:01	00:21
	19	Scope	Left flank	65	00:25	<00:01	00:01	00:05	<00:01	00:31